2

Dose Calculations of the Ru/Rh-106 CCA and CCB Eyes Applicators

Itzhak Orion and Emanuel Rubin
Ben-Gurion University of the Negev, Israel

1. Introduction

One of the tumors that radiotherapy can be implemented is the choroidal melanoma – eye cancer. Since it is possible to bring the radiation source into the tumor vicinity, the use of a sealed beta radiation source became an applicable treatment. A short range of radiation of few millimetres or less with a minimal radiation spread to the surrounding can be preferable. Since the eye is a very sensitive organ high dose radiation could seriously damage it and even to cause blindness. The sensitivity of the eye parts is – in a descending order - the lens, corona, conjunctiva, retina, optic nerve, therefore it is important to map the accurate absorbed dose to the eye during a treatment (Egbert et al., 1980). Medium and large sized tumors are vastly treated with ^{125}I applicators, and β^- ray applicators such as ^{106}Ru are in use for small- sized tumors in eyes. ^{106}Ru ophthalmic applicators have been used for close to fifty years in the treatment of choroidal melanoma. Sixteen standard models of ^{106}Ru applicators are currently manufactured by BEBIG GmbH, Germany (BEBIG, 2003). The form of these applicators is a spherically concave silver bowl with an inner radius of curvature between 12 and 14 mm, and a total shell thickness of 1 mm. Various shapes with diameters between 11.5 and 25.5 mm are available.

The radioactive layer is electrically deposited with an approximate thickness of 0.1 mm on the concave surface of a 0.2 mm thick silver target foil. This target foil is, in turn, deposited between the concave surface of a 0.7 mm thick layer of silver (rear) and the convex surface of a 0.1 μm thick layer of silver (window). The precise applicator measures were provided by the manufacturer, BEBIG GmbH.

The ^{106}Ru parent disintegrates via beta decay with peak energy of 39 keV to a radionuclide daughter, the ^{106}Rh. The primary contributor to therapeutic dose is the continuous spectrum of beta particles emitted from the decay of ^{106}Rh (half-life ~30 sec). ^{106}Rh disintegrates by beta decay that its mean beta energy is of about 1.4 MeV and maximum of 3.54 MeV to ^{106}Pd (stable).

Two main papers on the subject of Monte Carlo simulations of the Ru/Rh-106 applicators were previously published. In the paper by Sánchez-Reyes et al. dose distribution results using the PENELOPE code (Salvat et al., 1996) were presented in 1998 (Sanchez-Reyes et al., 1998). The study using the PENELOPE code lead to different results than presented in this work, due to new developments in the electron transport model that were implemented after the year 2005. Šolc recently published simulation results of the MCNPX code for a COB-type applicator only, and showed a good agreement between the simulated doses to measurements results (Šolc, 2008).

Dose measurements were carried out using three-dimensional scintillation dosimetry for CCX-type eye applicators, and isodose maps were obtained (Kirov et al. 2005). The measurements results were presented for 4 mm depth and higher only.

A high accuracy model for the simulations of the CCA-type and the CCB-type applicators in the one of the most updated Monte Carlo code for electrons, the EGS5, is presented in this chapter. The choice of the applicator type is made by the physician according to the size and depth of the treated tumor.

2. Materials and methods

The applicators are made of the ^{106}Ru isotope with half life of 373.59 days with maximum energy of 39 keV. The 39 keV beta rays of the Ru cannot escape the applicator window due to their short range in silver. In the simulation, therefore, the beta rays of the ^{106}Ru were not taken into account. The decay formulae are listed in Eq. (1). The daughter ^{106}Rh emits a continuum spectrum of beta of the following main energies: 1.51 MeV (79%), 0.97 MeV (9.7%), 1.27 MeV (8.4%). The ^{106}Rh and the ^{106}Ru properties are listed in Table 1. The overall continuum beta emission of the ^{106}Rh, shown in Figure 1, was fitted and programmed as an energy source distribution to the EGS user-code.

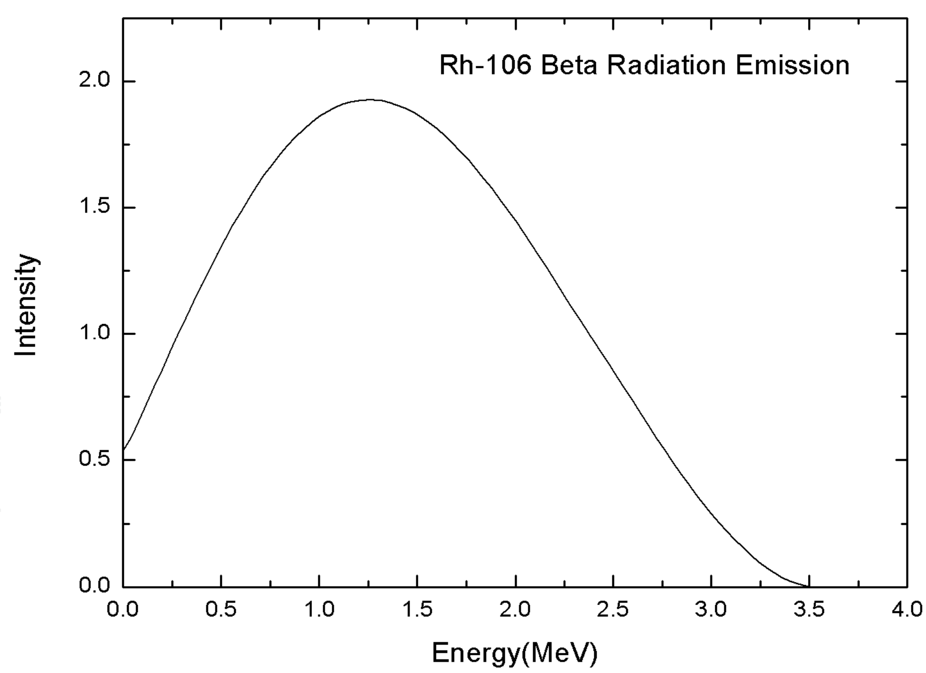

Fig. 1. The Ru-106 total beta emission spectrum used in the simulations [data was taken from JEF-PC 2.0 database (Konieczny , 1997)].

$$^{106}_{44}Ru \rightarrow ^{106}_{45}Rh + \beta^- + \bar{\nu}$$

$$^{106}_{45}Rh \rightarrow ^{106}_{46}Pd + \beta^- + \bar{\nu} \quad (1)$$

Radioisotope	^{106}Rh	^{106}Ru
Atomic number	45	44
Atomic mass	106	106
Half life	29.80 sec	373.15 day
Q-value (keV)	3541	39.40
Decay	β^-	β^-
Density (g cm^{-3})	12.4	12.2

Table 1. The beta source properties (From ENSDF - NNDC).

In Figs 2,3 the vertical cross-sectional view of each applicator are shown. The CCA-type applicator dimensions are: concave with a radius of 12.0 mm; Height h = 3.3 mm; The whole applicator diameter is 15.3 mm; The radioactive part diameter is 13.4 mm. Total applicator angle of 72.2° (2 x 36.1°); The radioactive part angle of 67.4° (2 x 33.7°).

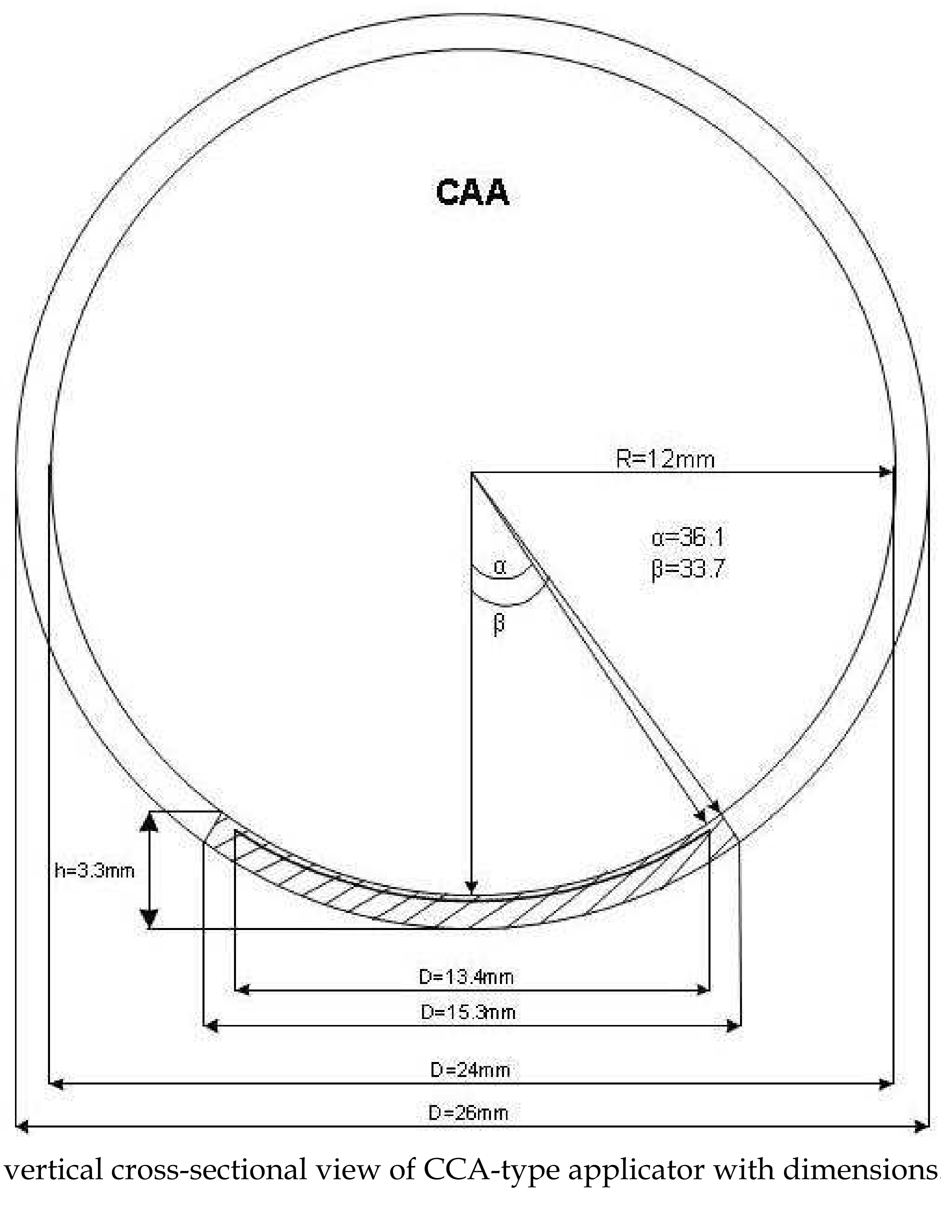

Fig. 2. The vertical cross-sectional view of CCA-type applicator with dimensions.

The CCB-type applicator dimensions are: concave with a radius of 12.0 mm; Height h = 5.4 mm; The whole applicator diameter is 20.0 mm; The radioactive part diameter is 18.2 mm. Total applicator angle of 101.8° (2 x 50.9°); The radioactive part angle of 97.8° (2 x 48.9°).

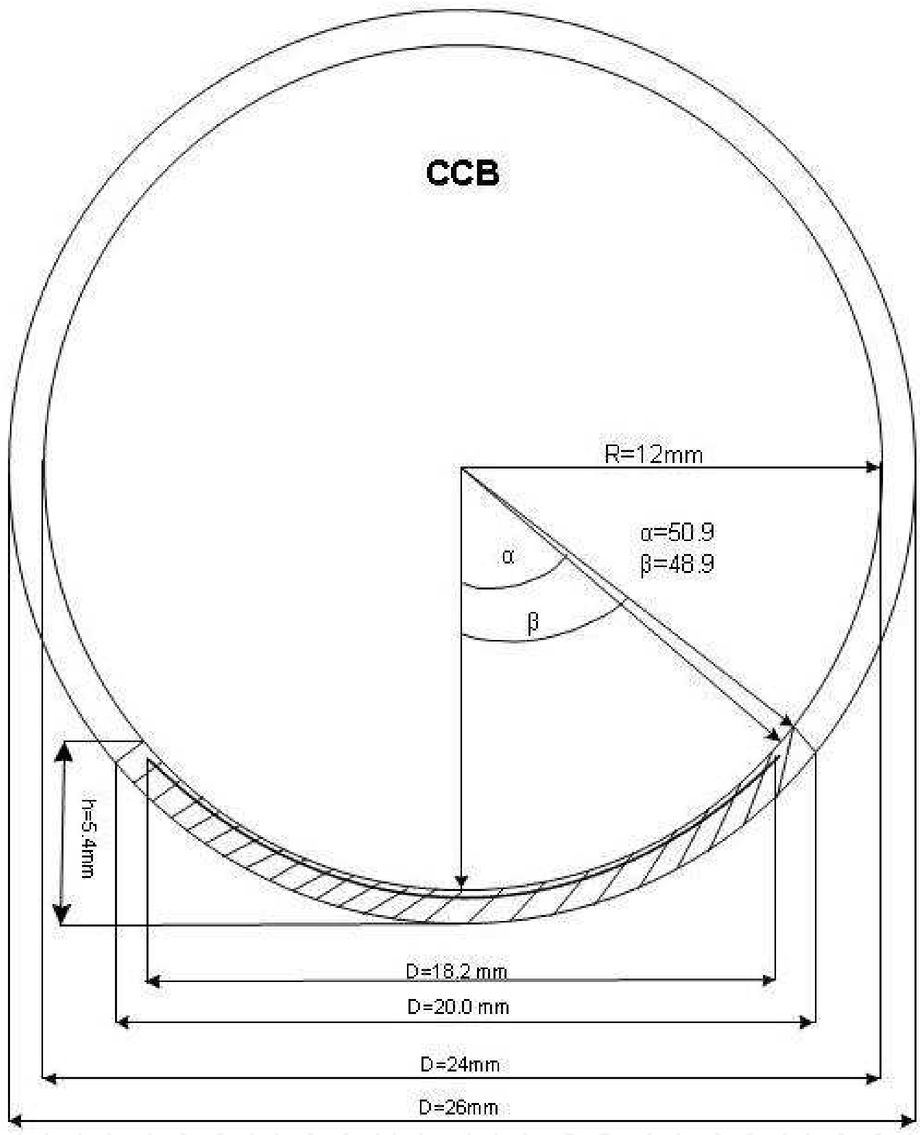

Fig. 3. The vertical cross-sectional view of CCB-type applicator with dimensions.

2.1 The beta emission area distribution

In order to distribute the beta emission source area on a concave surface, PDF (Probability Density Functions) were formulated using spherical functions. The total areas for the CCA-type and for the CCB-type are:

$$Total\ Area_{CCA} = r^2 \int_0^{2\pi} d\theta \int_0^{\frac{33.7\cdot\pi}{180}} \sin(\varphi)\,d\varphi = 0.336\pi r^2 \tag{2}$$

$$Total\ Area_{CCB} = r^2 \int_0^{2\pi} d\theta \int_0^{\frac{48.9\cdot\pi}{180}} \sin(\varphi) d\varphi = 0.543\pi r^2 \qquad (3)$$

Hence, after taking into account each case integration limits, the specific cumulative density functions (CDFs) are:

$$\begin{aligned} F(\theta,\varphi) &= r^2 \zeta_1 \theta \left(1 - \cos(\zeta_2 \varphi)\right) \\ F(\theta) &= 2\pi\zeta_1 \\ F(\varphi)_{CCA} &= \frac{180}{33.7}\arccos(\zeta_2) \\ F(\varphi)_{CCB} &= \frac{180}{48.9}\arccos(\zeta_2) \end{aligned} \qquad (4)$$

Where ζ notes a uniform random number in the range [0,1].

Each of the source positions on the surface were set to introduce an isotropic emission probabilities.

2.2 The Monte Carlo simulation code

The Monte Carlo method provides approximate solutions to a variety of mathematical problems by performing statistical sampling that rely on repeated random sampling. A computer calculates the results of simulated experiments. The method is used to resolve problems with no probabilistic content as well as those with inherent probabilistic structure, such as the interaction of nuclear particles with materials. It is particularly useful for complex problems that cannot be modelled by computer codes that use deterministic methods.

The EGS (Electron-Gamma Shower) code system is a general purpose package for the Monte Carlo simulation of the coupled transport of electrons and photons in an arbitrary geometry for particles with energies ranging from above a few keV up to several hundred GeV. The EGS5 is a FORTRAN open source program. Since the 1990s when the previous EGS4 code was released, it has been used in a wide variety of applications, particularly in medical physics, radiation measurement studies, and industrial development. The EGS5 code system (Hirayama et al. 2006) contains, among many other subprograms, four user-called subroutines: BLOCK SET, PEGS5, HATCH, and SHOWER. These routines call other subroutines in the EGS5 code, some of which call two user-written subroutines, HOWFAR and AUSGAB, which respectively define geometry, and scoring output. The EGS5 transport code for electrons is fundamentally different and advanced from the previous EGS4 code. The electron step in EGS5 is treated by splitting each step into two segments, and a scattering hinge is applied in between the segments (Bielajew & Wilderman, 2000). The user communicates with EGS5 by means of the subroutines mentioned above which enable him to access variables contained in various COMMON blocks. To use EGS5, the user must write a MAIN program and the subroutines HOWFAR and AUSGAB.

The Monte Carlo simulations were written using the EGS5 code system. The EGS5 Monte Carlo code system is a new generation of the EGS4 well validated code for photons and electrons transport. The EGS5 consists of newly developed pseudo-random generator, accurate low-energy photon fluorescence transitions and new algorithm for Bremsstrahlung radiation, which assure reliable results for radiation simulations studies. The EGS5 includes several tools, such as the CG-VIEW for geometry editing and as a viewer, and the PEGS5 editor for media cross sections definitions. All kinetic energy cut-offs were set to be at 1 keV along this study. The EGS5 is running under LINUX operating systems. A schematic flowchart to illustrate how the user is able to prepare a simulation in EGS5 is presented in Figure 4.

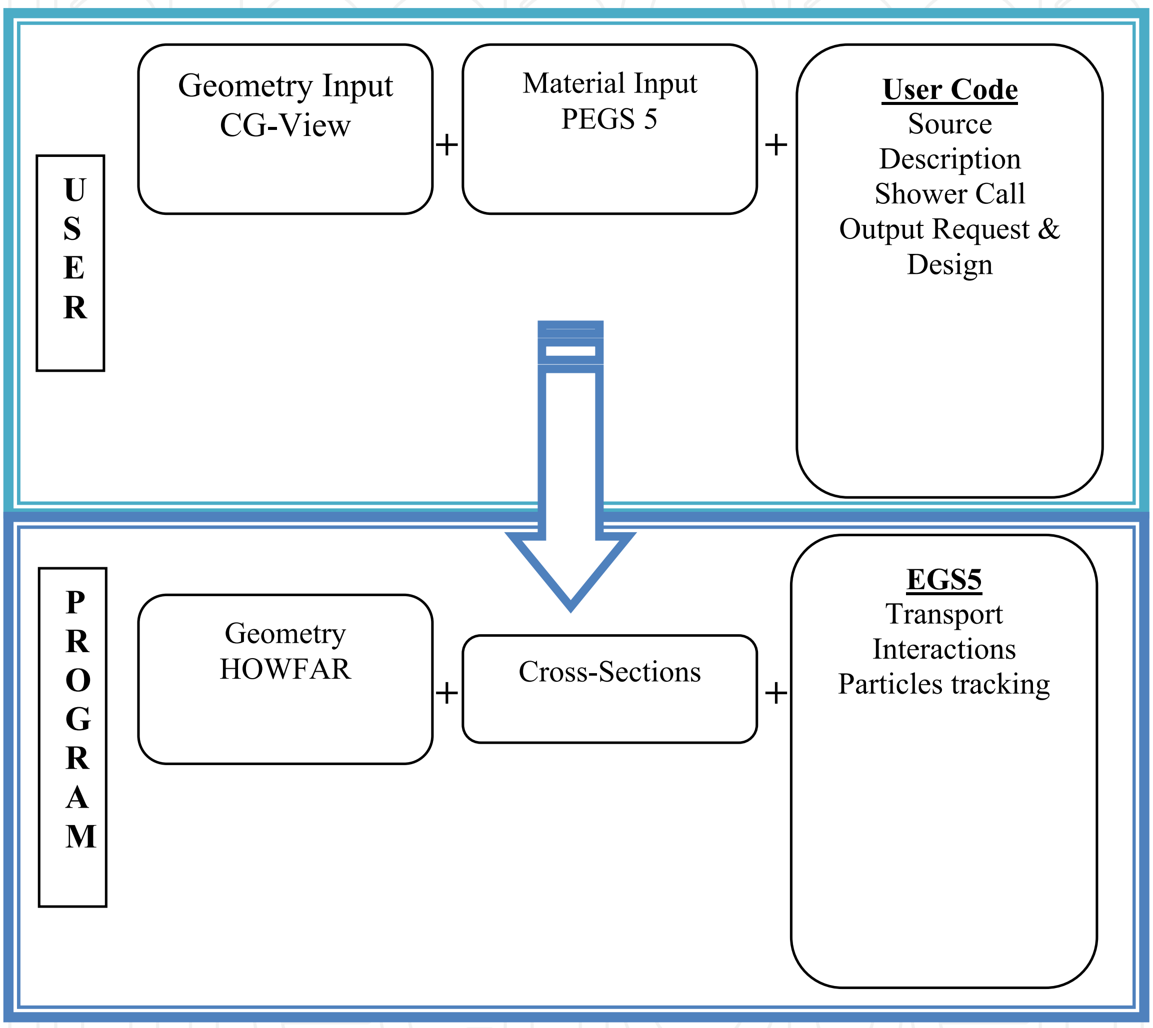

Fig. 4. The EGS5 code system schematic layout.

The detailed geometry of each applicator as described above was input and checked for the simulations using the CG-VIEW program, which is a complementary part of the EGS5 package. The media used in the simulations are: Ag and Ru for the applicator, soft tissue [based on ICRU44: tissue, soft ICRU Four-Component (ICRU – 44, 1989)] as the filling of the eye.

The CCA-type applicator simulation was visually inspected by tallying 200 primary electron tracks into the CG-VIEW program. The electron tracks results are shown in Figure 5 (the secondary photons lines were not represented). The basic structure of the electrons range and spread in the applicator and in the eye can be seen.

The simulations tallied energy deposition in 1 mm diameter spheres in order to calculate the absorbed dose. Each run, consist of 5 million histories, took about 25 hours on a PC computer (Intel® Pentium ® 1.60 GHz).

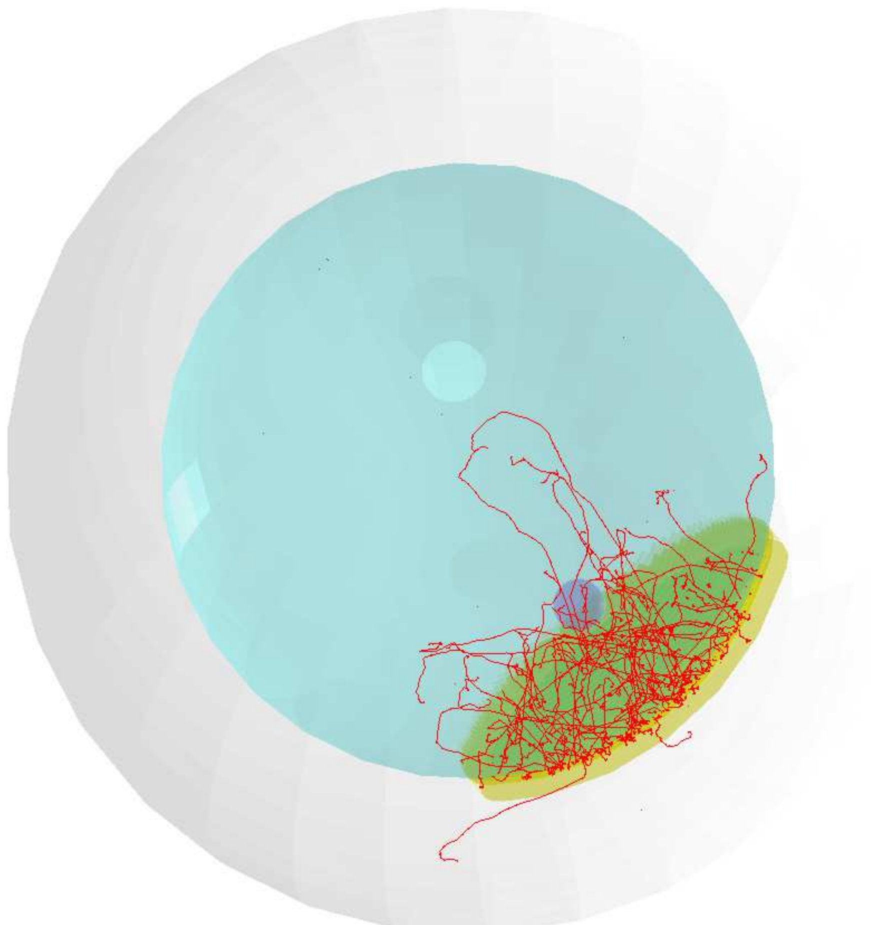

Fig. 5. Electron tracks from the simulated CCA-type applicator as presented by the CG-VIEW program.

3. Results and discussion

The results provided the dose delivered in a treatment of choroidal melanoma. The EGS5 depth dose results were compared to the BEBIG manufacturer results that were supplied with the applicators data sheets. The measured results were obtained from a 1 mm x 0.5 mm scintillator with an error of about 20 % (Fluhs et al., 1996). The measured results and the simulations results were both normalized to be 100 at 2 mm depth. The comparison for each applicator type is shown in Figure 6. The comparison showed mostly a good agreement between the measurements and the simulations results. The simulations statistical uncertainties were analyzed to be discussed in details in the conclusions section.

The results of the radial dose distributions in Figure 7 were obtained using another set of EGS5 Monte Carlo simulations. The absorbed dose was accumulated in 1 mm radius spherical unit-cells positioned around the eyeball center at a 11 mm radius across a perpendicular plan to the applicator. The 0° angle is at the closest position to the applicator concave center, where the dose was normalized to be of a value of 100. The radial dose for the CCA-type and for the CCB-type applicators showed a decrease of five orders of magnitude along a range of 120° (Figure 8).

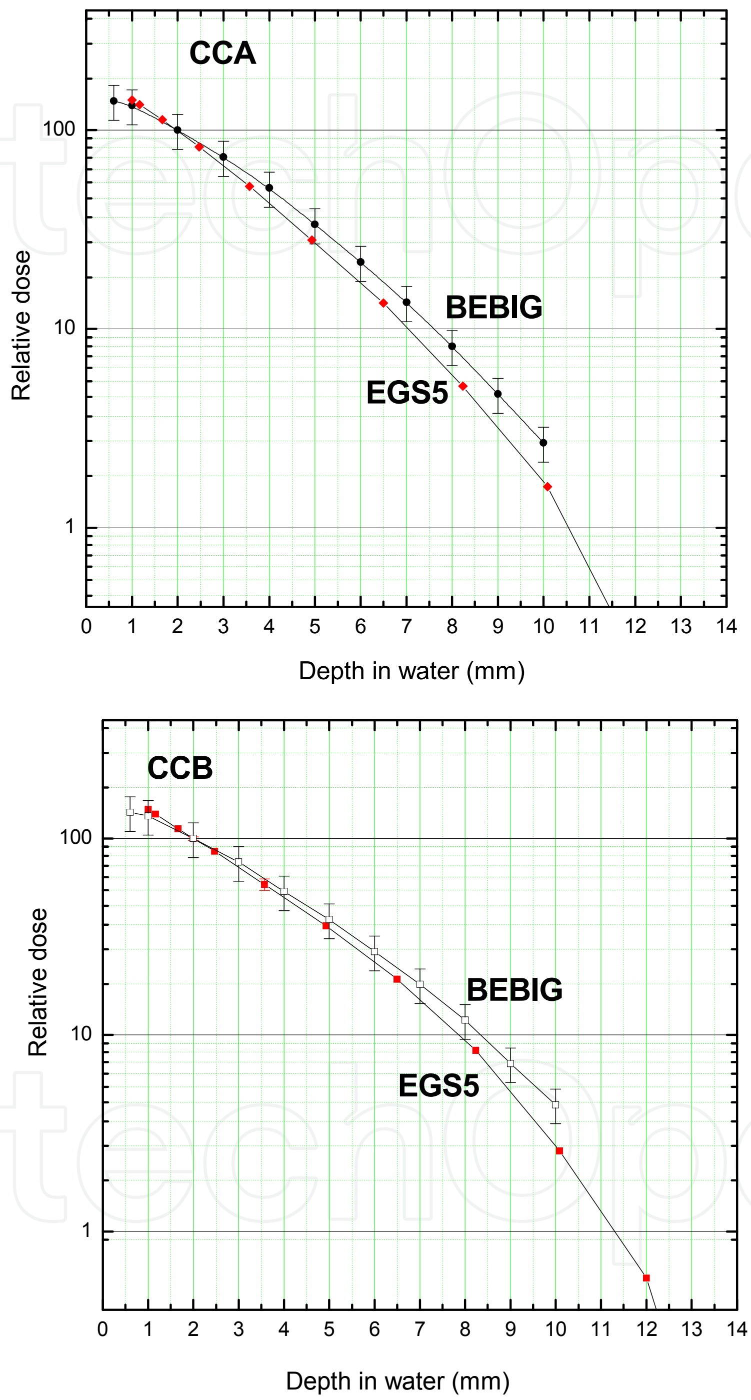

Fig. 6. Comparison of the dose versus depth in water measurements to simulations results for the CCA-type and for the CCB-type applicators.

The normalized absorbed dose (100 at 2 mm distance) along several plans at 2 mm to 8 mm above the applicators were obtained from the simulations, and plotted in Figure 7. The CCA-type dose is more flat even at lower plans compared to the CCB-type dose.

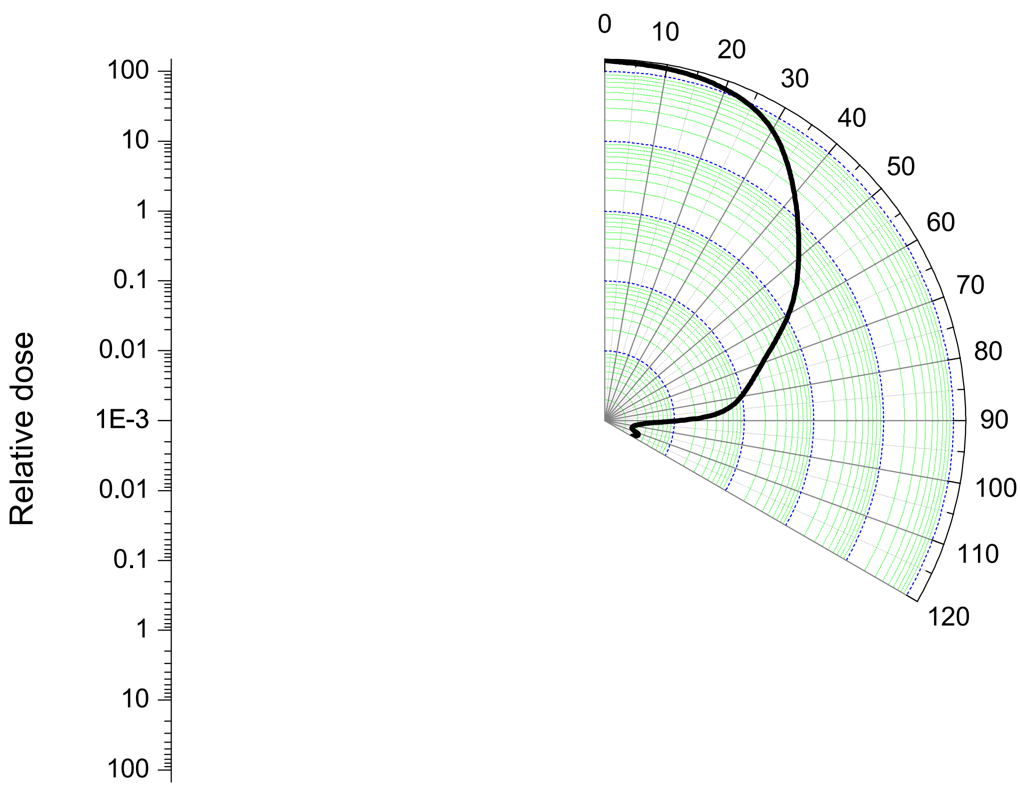

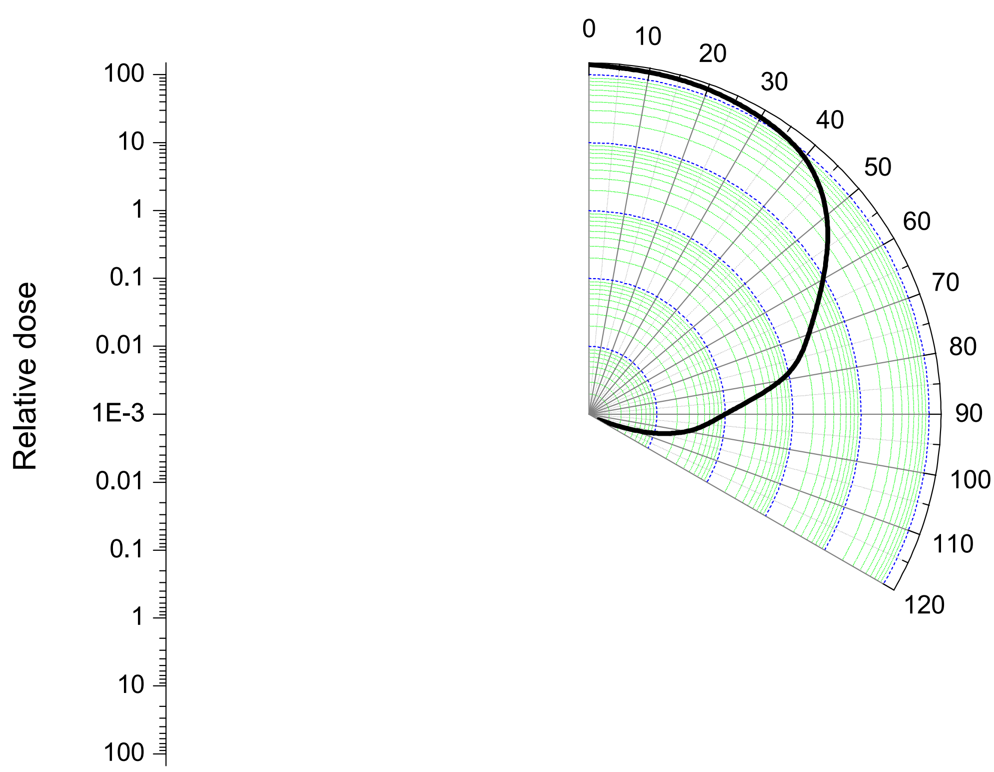

Fig. 7. The radial dose distributions in a 1 mm radius unit-cell moving around the eyeball center at a 5 mm radius across a perpendicular plane to the applicator.

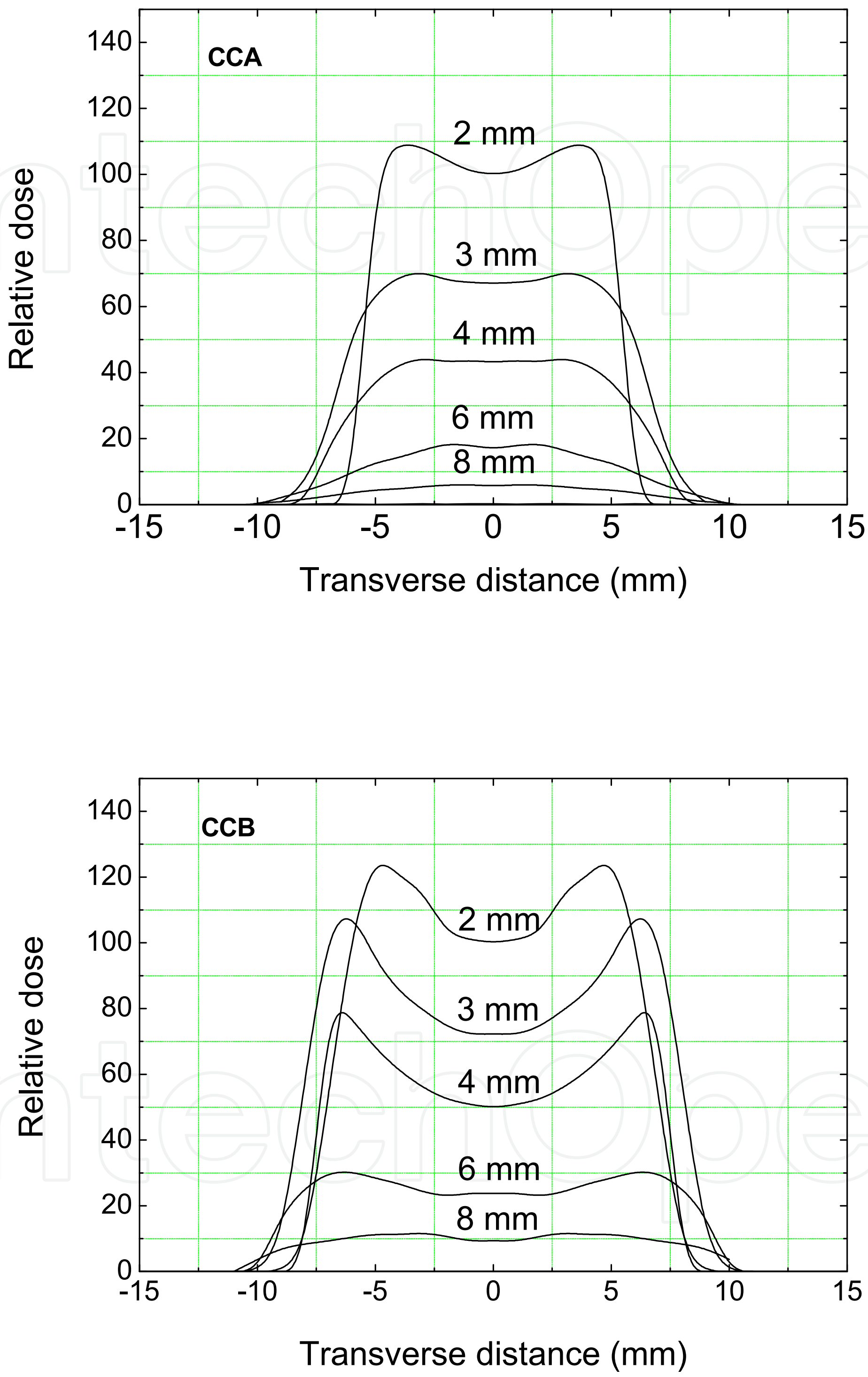

Fig. 8. The EGS5 normalized absorbed dose along several planes at 2 mm to 8 mm above the applicators.

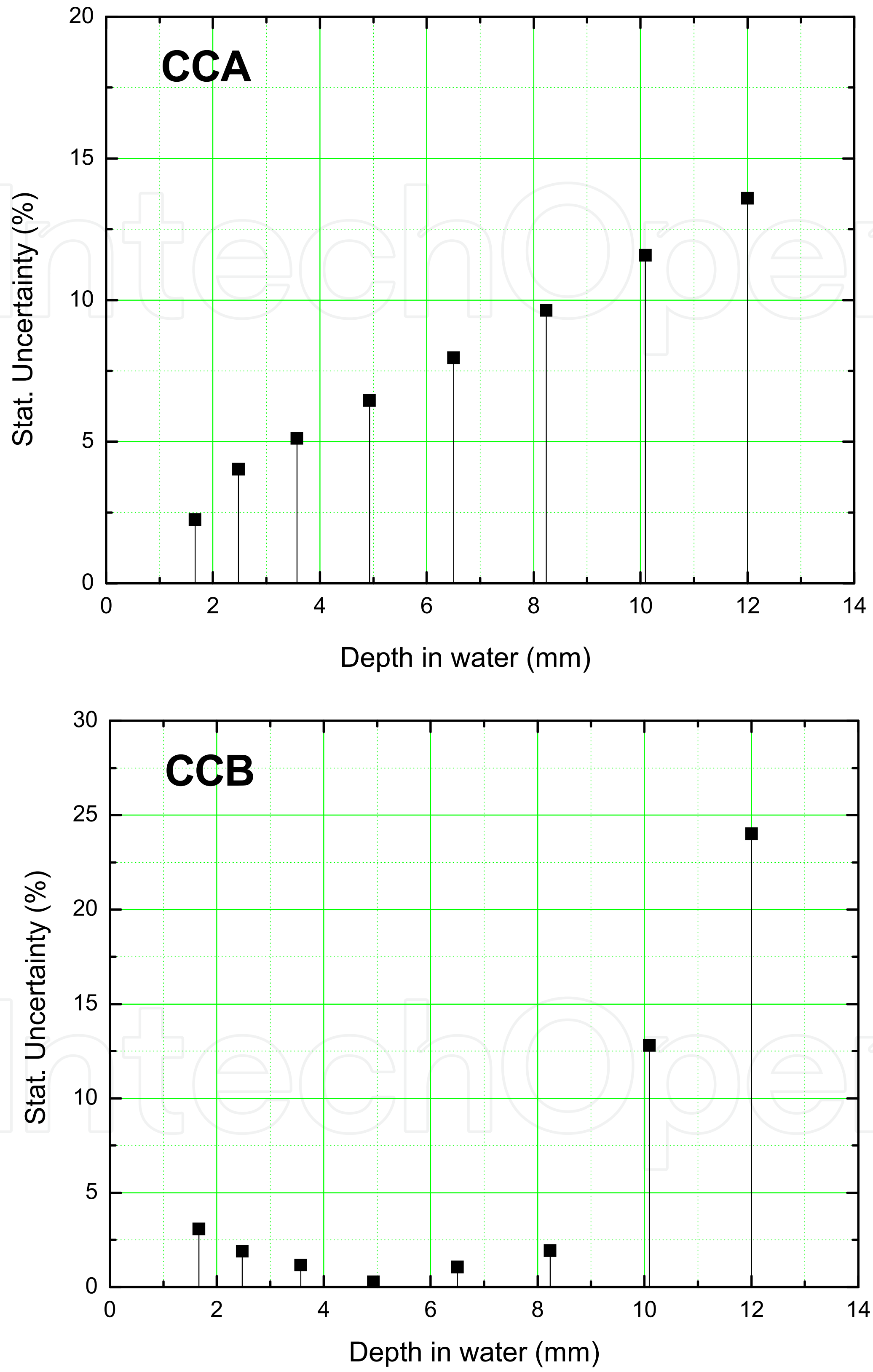

Fig. 9. The simulations statistical uncertainties versus depth in water for CCA-type and for CCB-type applicators.

Depth (mm)	EGS5 Dose (norm. at 2 mm)	PENELOPE Dose (norm. at 2 mm)	Difference (%)
1.0	142.1	144.7	1.8
1.5	113.0	117.0	3.5
2.0	100.0	100.0	0.0
2.5	82.3	78.7	4.4
3.0	67.7	74.5	9.5
3.5	52.1	57.4	9.8
4.0	44.5	40.4	9.5
5.0	27.1	25.5	5.8
6.0	18.3	17.0	7.4
6.5	13.5	12.8	5.6
7.0	10.7	10.6	0.7
8.0	6.8	6.8	0.1

Table 2. Comparison of the EGS5 simulation depth dose results from this study to PENELOPE results after normalization (taking from Sanchez-Reyes, 1998): a) CCA-type Applicator.

Depth (mm)	EGS5 Dose (norm. at 2 mm)	PENELOPE Dose (norm. at 2 mm)	Difference (%)
1.0	140.9	131.9	6.6
1.5	111.7	114.9	2.8
2.0	100.0	100.0	0.0
2.5	85.9	89.4	3.9
3.0	72.6	78.7	8.1
3.5	58.3	70.2	18.6
4.0	51.2	61.7	18.6
5.0	34.9	46.8	29.2
6.0	24.8	40.4	48.0
6.5	19.2	29.8	43.3
7.0	15.6	25.5	48.4
8.0	10.4	17.0	47.9

Table 3. Comparison of the EGS5 simulation depth dose results from this study to PENELOPE results after normalization (taking from Sanchez-Reyes, 1998): b) CCB-type Applicator.

3. Conclusion

The dose calculations were carried out for two main applicator types, CCA-type and CCB-type, using the EGS5. The Monte Carlo simulations results obtained in this study are close to the manufacturer's measured data. Comparison to measurements showed a difference of about 10% (CCB) and 20% (CCA) at 5 mm depth. The dose statistical uncertainties in the calculations show that for an amount of 10% for the CCA-type and an uncertainty of 2.5%

for the CCB-type, at 8.5 mm depth. However, in both applicators the dose reduction was found over one magnitude up to a distance of 7.5 mm.

The simulation statistical uncertainties versus depth are shown in Figure 9. Different depth dependence was found for CCA-type applicator compared to CCB-type applicator. The CCA-type uncertainties are constantly increasing with depth, whilst the CCB-type statistical uncertainties were not gradually increased.

This different behavior can be explain by the nature of the active area radioactive distribution, when in CCB-type the angle of the active area is much vast resulting a higher flux toward the central axis up to a distance of 8.5 mm. The EGS5 statistical uncertainties assessments showed that the CCB-type source might be proffered, due to low uncertainties along the treatment range.

Since the same applicators dose was simulated in a previous Monte Carlo simulations study using a different Monte Carlo code, the PENELOPE (Sanchez-Reyes et al., 1998), it was interesting to examine the difference of the dose results. The relative dose versus depth in water from the EGS5 results was compared to the relative dose from PENELOPE after normalizing the values to be 100 at 2 mm depth. The comparison was preformed for the CCA-type and for the CCB-type applicators, as listed in Tables 2,3. Even the CCA-type applicator's external diameter of the active area is different from the current work (15.5 mm instead of 15.3 mm), the results showed up to 10 % only dose difference that can be explained by the statistical uncertainty. The CCB-type comparison results showed increasing dose difference toward 49 % along the 8 mm depth in water. The EGS5 showed always lower dose compared to the PENELOPE results in the CCB-type applicator, which is might be expressed due to the different electron transport of the EGS5 code. The CCA-type applicator results of the EGS5 study showed transverse dose profile that has a clear shape difference in Figure 6 compared to the PENELOPE published results [(Sanchez-Reyes et al., 1998) see Figure 4]. It can be seen that EGS5 could follow fine profile structure of the CCA-type, while PENELOPE could result that fine structure in the CCB-type that causes a more non smooth shape.

This study showed the potential of using Monte Carlo simulations in order to calculate the radiation dose delivered to the eye in high accuracy in a short computing time, which may assist the choice of applicator type for every individual treatment.

4. Acknowledgment

The authors would like to thank Professor Yaakov Peer from Hadassah University Hospital in Jerusalem, Israel. We thank BEBIG Company for the applicators data and details supplied that assist to perform the research.

5. References

BEBIG; (2003). Ruthenium eye applicator customer information: introduction of the new NIST-calibrated dosimetry introduction of the new PTB - calibrated activity measurement. Berlin.
Available from http://www.bebig.eu/products/ophthalmic.html

Bielajew A. F. & Wilderman S. J. (2000). Innovative Electron Transport Methods in EGS5, Proceedings of the 2nd International Workshop on EGS, KEK, Japan (KEK Proceedings 2000-20).

Egbert P. R.; Fajardo L.F.; Donaldson S. S. & Moazed K. (1980). Posterior ocular abnormalities after irradiation for retinoblastoma: a histopathological study, *Br. J. Ophthalmol*, Vol. 64 pp. 660-665

ENSDF, "Evaluated Nuclear Structure Data File" National Nuclear Data Center, Brookhaven National Laboratory, Upton, NY 11973-5000
Available from http://www.nndc.bnl.gov/

Fluhs D.; Heintz M.; Indenkampen F.; Wieczorek C.; Kolanoski H. & Quast U. (1996). Direct reading measurement of absorbed dose with plastic scintillators—the general concept and applications to ophthalmic plaque dosimetry, *Medical Phys*ics Vol. 23, pp. 427–434

Hirayama H.; Namito Y.; Bielajew A. F.; Wilderman S. J. & Nelson W. R. (2006). *The EGS5 code system* SLAC-R-730 / KEK Report 2005-8

ICRU - 44 (1989). *Tissue Substitutes in Radiation Dosimetry and Measurement*, Report 44 of the International Commission on Radiation Units and Measurements, Table 2 (Bethesda, MD)

Kirov A.S.; et al. (2005). The three-dimensional scintillation dosimetry method: test for a ^{106}Ru eye plaque applicator, *Phys Med Biol.* Jul 7; 50(13):3063-81

Konieczny M. et al. (1997). JEF-PC Version 2.0, *Proc. Int. Conf. on Nuclear Data for Science and Technology*, Trieste, Italy, May 1997, p. 1063

Salvat F.; FernaÂndez-Varea J. M.; Baro Â. J. & Sempau J (1996). *PENELOPE, an algorithm and computer code for Monte Carlo simulation of electron photon showers*, CIEMAT Report n. 799. Madrid

Sanchez-Reyes A.; Tello J. J.; Guix B. & Salvat F. (1998). Monte Carlo calculation of the dose distributions of two ^{106}Ru eye applicators, *Radiotherapy and Oncology* 49, pp. 191-196

Šolc J. (2008). Monte Carlo calculation of the dose water of a COB-type ophthalmic plaque, Third McGill International Workshop, *Journal of Physics: Conference Series 102*

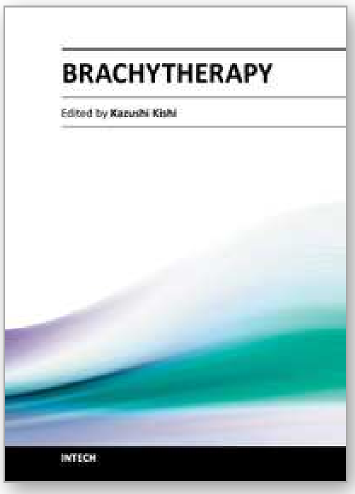

Brachytherapy

Edited by Dr. Kazushi Kishi

ISBN 978-953-51-0602-9
Hard cover, 128 pages
Publisher InTech
Published online 25, April, 2012
Published in print edition April, 2012

Importance of brachytherapy is currently increasing in cancer therapy. In brachytherapy each treatment is best fitted by physician's' hand, and appropriate arrangement and selection of radiation sources facilitates the fitting. This book is full of essences to make a breakthrough in radiation oncology by brachytherapy. I hope this book will encourage all people related. Contents 1: problem of currently popular dosimetric method; 2: Monte Carlo dose simulation of ruthenim-106/rhodium-106 eyes applicators; 3. Progress in Californium-252 neutron brachytherapy; 4. Clinical aspect of endobronchial brachytherapy in central airway tumor obstruction; 5. Review from principle and techniques of Iodine-125 production at nuclear reactor plant to their clinical practive in prostate cancer treatment; 6. Stereotactic Brachytherapy for Brain Tumors using Iodine-125 seed; 7. A brachytherapy procedure with organ-sparing hyaluronate gel injection for safe and eradicative reirradiation.